

A small molecule–kinase interaction map for clinical kinase inhibitors

Miles A Fabian^{1,3}, William H Biggs III^{1,3}, Daniel K Treiber^{1,3}, Corey E Atteridge¹, Mihai D Azimioara^{1,2}, Michael G Benedetti^{1,3}, Todd A Carter¹, Pietro Ciceri¹, Philip T Edeen¹, Mark Floyd¹, Julia M Ford¹, Margaret Galvin¹, Jay L Gerlach¹, Robert M Grotzfeld¹, Sanna Herrgard¹, Darren E Insko¹, Michael A Insko¹, Andiliy G Lai¹, Jean-Michel L elias¹, Shamal A Mehta¹, Zdravko V Milanov¹, Anne Marie Velasco¹, Lisa M Wodicka¹, Hitesh K Patel¹, Patrick P Zarrinkar¹ & David J Lockhart¹

Kinase inhibitors show great promise as a new class of therapeutics. Here we describe an efficient way to determine kinase inhibitor specificity by measuring binding of small molecules to the ATP site of kinases. We have profiled 20 kinase inhibitors, including 16 that are approved drugs or in clinical development, against a panel of 119 protein kinases. We find that specificity varies widely and is not strongly correlated with chemical structure or the identity of the intended target. Many novel interactions were identified, including tight binding of the p38 inhibitor BIRB-796 to an imatinib-resistant variant of the ABL kinase, and binding of imatinib to the SRC-family kinase LCK. We also show that mutations in the epidermal growth factor receptor (EGFR) found in gefitinib-responsive patients do not affect the binding affinity of gefitinib or erlotinib. Our results represent a systematic small molecule–protein interaction map for clinical compounds across a large number of related proteins.

Protein kinases are critical components of cellular signal transduction cascades. They are directly involved in many diseases, including cancer and inflammation, and have become one of the most important target classes for drug development^{1,2}. The approval of imatinib (Gleevec) for chronic myeloid leukemia (CML), and gefitinib (Iressa) and erlotinib (Tarceva) for non-small cell lung cancer (NSCLC) has provided proof-of-principle that small molecule kinase inhibitors can be effective drugs. Over 30 kinase inhibitors are currently in clinical development, and many more are in preclinical studies. The vast majority of these compounds target the kinase ATP site, and because all of the more than 500 protein kinases identified in the human genome have an ATP site³, there is great potential for cross-reactivity. Compounds must be tested experimentally against many kinases to assess molecular specificity and to identify off-target interactions^{4,5}. Binding specificity and affinity are not readily predicted based on available sequence or structural information, and conventional profiling methods based on *in vitro* activity are limited by the difficulty of building and running large numbers of kinase activity assays.

We describe an experimental approach to assessing the specificity of kinase inhibitors that directly and quantitatively measures binding to the ATP site. Importantly, the method does not require chemical linking, labeling or immobilization of tested compounds (**Supplementary Notes** online). The approach circumvents many of the difficulties of conventional enzyme activity assays and allows rapid

development and efficient use of assays for large numbers of kinases. We have applied the technology to develop assays for 113 distinct protein kinases and six of the clinically observed imatinib-resistant variants of the ABL kinase, and have determined quantitative binding profiles for 20 kinase inhibitors, including staurosporine, imatinib, gefitinib and 14 compounds which are now or have been in clinical development. We have also assessed the effect of nine recently identified gefitinib-sensitizing EGFR mutations^{6,7} on the interaction of EGFR with eight known EGFR inhibitors, including gefitinib and erlotinib. The data constitute a small molecule–kinase interaction map and represent a systematic exploration of binding behavior of clinical compounds across a large protein class.

RESULTS

Binding assays for small molecule–kinase interactions

The approach uses ATP site–dependent competition binding assays (**Fig. 1a**)⁸. The key assay components are human kinases expressed as fusions to T7 bacteriophage and a small set of immobilized probe ligands that bind to the ATP site of one or more kinases. The small set of immobilized ligands is used to build the assays, but the ‘free’ test compounds (e.g., the 20 molecules profiled here) are not linked, labeled or immobilized. The kinases used in the assays can be viewed as fusion proteins that are tagged to facilitate expression, purification and detection. In this scheme the T7 phage particle is not unlike more

¹Ambit Biosciences, 4215 Sorrento Valley Blvd., San Diego, California 92121, USA. ²Present addresses: Genomics Institute of the Novartis Research Foundation, 10675 John Jay Hopkins Dr., San Diego, California 92121, USA (M.D.A.), Buck Institute, 8001 Redwood Blvd., Novato, California 94945, USA (M.G.B.), Seattle Biomedical Research Institute, 307 Westlake Ave. N., Ste. 500, Seattle, Washington 98109, USA (J.L.G.) and Metabasis Therapeutics, 9390 Towne Centre Dr., San Diego, California 92121, USA (M.A.I.). ³These authors contributed equally to this work. Correspondence should be addressed to D.J.L. (dlockhart@ambitbio.com) or P.P.Z. (pzarrinkar@ambitbio.com).

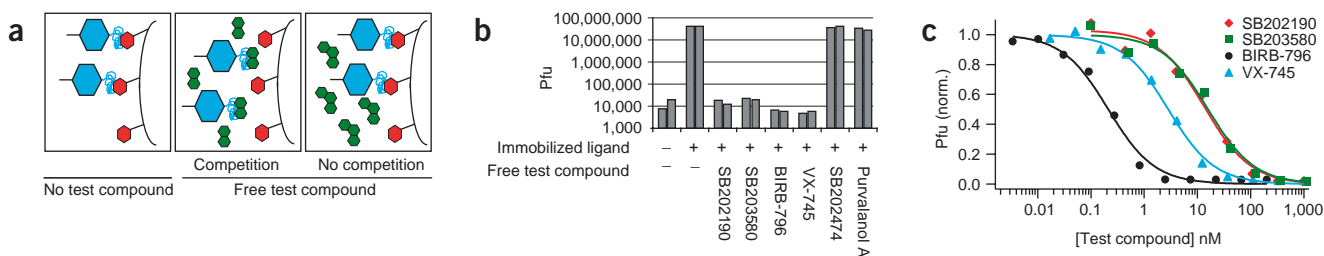


Figure 1 Competition binding assay for measuring the interaction between unlinked, unmodified ('free') small molecules and kinases. **(a)** Schematic overview of the assay. The phage-tagged kinase is shown in blue, 'free' test compound in green and immobilized 'bait' ligand in red. **(b)** Binding assay for p38 MAP kinase. The immobilized ligand was biotinylated SB202190. The final concentration of test compounds during the binding reaction was 10 μ M. **(c)** Determination of quantitative binding constants. Binding of tagged p38 to immobilized SB202190 was measured as a function of unlinked test compound concentration. Tagged p38 kinase was quantified by real-time quantitative PCR and the results normalized. Representative curves are shown, and average binding constants from at least two independent experiments are listed in **Supplementary Table 4** online.

conventional protein tags such as glutathione S-transferase or green fluorescent protein, except that it renders the attached protein amplifiable and amenable to very sensitive and versatile detection. Kinases that have been cloned into the phage vector can be produced rapidly by simply growing phage in *Escherichia coli*. T7 phage replication leads to lysis of the bacterial host, and lysates containing properly folded, tagged kinases are used directly in the assay with no need for conventional protein purification. The small number of immobilized small molecule ligands used to build the assays bind kinases with high affinity ($K_d < 1 \mu$ M), and were amenable to attachment of biotin through a flexible chemical linker. For the assay, tagged kinases and immobilized 'bait' ligands were combined with the 'free' test compound (**Fig. 1a**). If the 'free' test compound binds the kinase and directly or indirectly occludes the ATP site, fewer protein molecules bind the immobilized ligand on the solid support. If the 'free' test compound does not bind the kinase, tagged proteins are able to bind to the modified solid support. The results are read out by quantifying the amount of fusion protein bound to the solid support, which is accomplished with extraordinary sensitivity by either traditional phage plaque assays or by quantitative PCR (qPCR) using the phage DNA as a template. Both quantitation methods enable near single-molecule protein detection, allowing us to accurately detect and 'count' as few as 10–100 tagged protein molecules.

To test our new approach, we initially built an assay for p38 MAP kinase. p38 is activated in response to extracellular signals and regulates the production of pro-inflammatory cytokines⁹. This kinase is considered an excellent target for inflammation, and a number of p38 inhibitors are in clinical trials⁹. Building the assay required tagged p38 protein and an immobilized ligand that binds the p38 ATP site. To produce tagged p38, we cloned the coding region for p38 α into the phage genome in-frame with the gene encoding the major T7 capsid protein. We chose as an immobilized ligand SB202190, a pyridinyl imidazole that was one of the first p38 inhibitors described (**Table 1**; see **Supplementary Table 1** online for compound structures)¹⁰. Biotin with a flexible linker was chemically attached to SB202190 and the biotinylated compound immobilized on streptavidin-coated magnetic beads¹¹. Tagged p38 was found to bind to beads on which SB202190 had been immobilized, but not to beads lacking the ligand (**Fig. 1b**). Phage with no displayed protein did not bind to beads with or without SB202190 (data not shown). Binding to the solid support is therefore dependent on both the immobilized ligand and on the displayed kinase.

Six different free (unlinked) compounds were tested for the ability to compete with the interaction between p38 and immobilized

SB202190: SB202190 (without biotin modification); SB203580 (a pyridinyl imidazole closely related to SB202190) (**Table 1**)^{10,12}; SB202474 (a pyridinyl imidazole that does not bind p38)¹⁰; BIRB-796 (**Table 1**)¹³; VX-745 (**Table 1**)¹⁴; and purvalanol A (a cyclin-dependent kinase 2 inhibitor)¹⁵. Competition with unmodified SB202190, SB203580, BIRB-796 and VX-745 decreased by 1,000-fold or more the amount of tagged p38 bound to the solid support, whereas neither SB202474 nor purvalanol A had an effect (**Fig. 1b**). Because BIRB-796 binds predominantly in a position adjacent to the ATP site and affects the conformation of the ATP site indirectly¹³, whereas SB202190, SB203580 and VX-745 bind directly in the ATP site, we can conclude that the assay can detect allosteric as well as direct binding interactions (**Supplementary Notes** online). To determine the affinity of the interactions, we quantified the amount of tagged p38 bound to the solid support as a function of free test compound concentration (**Fig. 1c**). The binding constants measured in this manner agree well with published values

Table 1 Kinase inhibitors for which specificity profiles were determined

Inhibitor	Primary targets ^a	Status ^a
Staurosporine	Pan-inhibitor	Research compound
SB202190	p38 α	Research compound
SB203580	p38 α	Research compound
VX-745	p38 α	Phase 2 (discont.)
BIRB-796	p38 α	Phase 3
SP600125	JNK	Research compound
Imatinib	ABL, KIT, PDGFR	Approved
Gefitinib	EGFR	Approved
Erlotinib	EGFR	Approved
CI-1033	EGFR subfamily	Phase 2
GW-2016	EGFR, ERBB2, ERBB4	Phase 3
EKB-569	EGFR, ERBB2	Phase 2
ZD-6474	VEGFR2, EGFR	Phase 2
Vatalanib/PTK-787	VEGFR2	Phase 3
SU11248	VEGFR2, PDGFR, FLT3, KIT	Phase 3
MLN-518	FLT3	Phase 1
LY-333531	PKC β	Phase 3
BAY-43-9006	RAF1	Phase 3
Roscovitine/CYC202	CDK2	Phase 2
Flavopiridol	CDK1, CDK2, CDK4	Phase 2 (discont.)

^aSource: Pharamaprojects database, V5 (PJB Publications, <http://www.pjbpubs.com>).

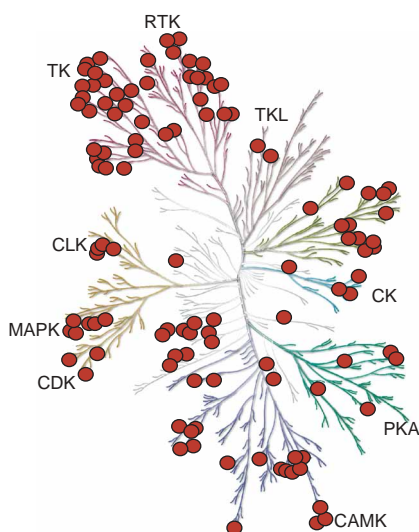


Figure 2 Panel of binding assays for 113 different protein kinases. Each kinase represented in the assay panel is marked with a red circle. Gene symbols for kinases in the panel are shown in **Figure 5**, as well as in **Supplementary Table 4** online. The kinase dendrogram was adapted³, and is reproduced with permission from *Science* and Cell Signaling Technology, Inc. (<http://www.cellsignal.com>). With sponsorship by Cell Signaling Technology and Sugen, the figure was originally presented as a poster in *Science* to accompany the first analysis of the complete human kinome. TK, nonreceptor tyrosine kinases; RTK, receptor tyrosine kinases; TKL, tyrosine kinase-like kinases; CK, casein kinase family; PKA, protein kinase A family; CAMK, calcium/calmodulin dependent kinases; CDK, cyclin dependent kinases; MAPK, mitogen-activated protein kinases; CLK, CDK-like kinases.

(**Supplementary Table 2** online). These results demonstrate that the new binding assay correctly discriminates between compounds that bind to the kinase and those that do not, and yields accurate binding constants.

Assays for 113 distinct protein kinases

To expand the approach, we produced tagged versions of additional human kinases. We have so far cloned into the phage vector 440 of the ~518 protein kinases in the human genome³. To develop additional assays, we next identified a small set of molecules that could be used as immobilized ligands. To avoid the need to find a unique ligand for each kinase, we sought molecules that bind with high affinity to the ATP site of multiple kinases. One molecule with these characteristics is staurosporine (**Table 1**)¹⁶. Biotinylated staurosporine was synthesized, immobilized and tested for binding to each of the 440 tagged kinases. To be considered for inclusion in the assay panel, a kinase was required to bind staurosporine-derivatized beads but not beads without ligand. Furthermore, binding had to be suppressed at least 100-fold when 10 μM staurosporine (not biotinylated) was included as a free test compound in the competition assay. With staurosporine as the immobilized ligand, these criteria were met for 51 kinases. The panel was expanded to 113 distinct protein kinases by testing SB202190 and additional immobilized compounds against our entire collection of tagged kinases and applying the same criteria as for staurosporine (**Fig. 2**). Kinases from all the major subfamilies are represented in the panel, and any known or potential kinase inhibitor can be tested for binding against the entire set of assays in a single experiment without the need for chemical modification. To validate the assays, we have shown that there is a very high correlation between inhibitor binding

affinity measured in the competition assays and inhibition of enzymatic activity measured in traditional enzyme or cell-based assays, and that this high correlation is observed for both known and novel interactions and for known and novel inhibitors (**Supplementary Tables 2 and 3**; see **Supplementary Notes** online for details).

Specificity profiles for clinical kinase inhibitors

There are currently over 30 kinase inhibitors in clinical trials or approved for use in humans. The particular set of kinases inhibited by a compound may profoundly affect therapeutic usefulness, yet for most molecules specificity has been determined against only relatively small sets of kinases^{13,17–27}. We systematically screened a set of well-known kinase inhibitors against the entire panel of 113 different kinases. Twenty compounds representing a diversity of chemical scaffolds and targeting a variety of kinases (**Table 1**; see **Supplementary Table 1** online for compound structures) were profiled in two steps. First, a primary screen against the entire kinase panel was performed at a compound concentration of 10 μM . Second, quantitative binding constants were determined for each hit in the primary screen (**Supplementary Table 4**; in this table blank fields indicate compound/kinase combinations for which no evidence of binding was observed at 10 μM in the primary screen).

The results show that molecular specificity varies widely among these known inhibitors (**Fig. 3**). Staurosporine is known to be a highly promiscuous inhibitor of many different kinases, and indeed binds to 104 of the 113 kinases with affinities fairly evenly distributed from 20 pM to ~7 μM (**Fig. 4**; **Supplementary Table 4** online). Among the compounds that have been in clinical trials, several, such as SU11248, bind to many kinases, whereas others, such as Vatalanib (also known as PTK-787) and GW-2016, bind very few kinases in addition to their known, primary targets. For most of the compounds tested here, the tightest interaction is with the kinase or kinases they were optimized to inhibit, but the difference in affinity between the primary target or targets and other kinases varies substantially (**Fig. 4**). For BIRB-796, VX-745, erlotinib, GW-2016 and SU11248, there is at least a tenfold difference in affinity between intended targets and off-targets, whereas for SP600125, EKB-569 and ZD-6474 there is less than a twofold difference (**Supplementary Table 4** online). This suggests that efforts to optimize kinase inhibitor potency against a particular target have been generally successful, but that it may be possible and even necessary to improve the ability of some compounds to discriminate between intended targets and off-targets.

Specificity can vary substantially even among compounds that are based on the same chemical scaffold or that target the same kinase. For example, the five quinazoline-class and quinoline-class EGFR inhibitors (**Supplementary Table 1** online) range from highly specific to quite promiscuous (**Fig. 3**; **Supplementary Table 4** online). GW-2016 binds only STK10 and SLK (in addition to EGFR and ERBB2), both of them fairly weakly ($K_d > 1 \mu\text{M}$), and is an example of an inhibitor that targets one kinase subfamily with exquisite specificity. EKB-569, in contrast, binds 56 of the 113 kinases, several of them with affinities almost equal to that for EGFR. Specificity also does not appear to be simply determined by the particular targeted kinase. For example, there are specific as well as promiscuous compounds among the EGFR inhibitors, as outlined above, and among the vascular endothelial growth factor receptor (VEGFR)2 inhibitors. Vatalanib binds only four kinases in addition to VEGFR2, whereas SU11248 and ZD-6474 bind 73 and 43 additional kinases, respectively (**Fig. 3**; **Supplementary Table 4** online). These results illustrate that specificity is not dictated by the general chemical scaffold of an inhibitor, or by the primary, intended kinase target.

There are many examples of off-targets that are not closely related by sequence and function to the primary, intended target. Many compounds considered tyrosine kinase inhibitors also bind to serine-threonine kinases, and serine-threonine kinase inhibitors frequently bind to tyrosine kinases (Table 1 and Fig. 3). Examples include the p38 inhibitors VX-745 and BIRB-796, which are chemically unrelated to each other but bind a number of tyrosine kinases, and the receptor tyrosine kinase inhibitors SU11248 and EKB-569, both of which bind a number of serine-threonine kinases. A meaningful assessment of specificity, therefore, cannot be achieved by testing only against kinases within the same subfamily. Even screening against a small number of representatives of multiple kinase families can be misleading. For example, CI-1033 was previously shown to be highly active against three members of the EGFR family, but to have no activity against seven other enzymes representing receptor tyrosine kinases, protein kinase C and cyclin-dependent kinases²¹. This led to the conclusion that CI-1033 is highly specific. The binding profile against a much larger panel shows, however, that CI-1033 binds at least 36 different kinases and is among the more promiscuous compounds (Fig. 3; Supplementary Table 4 online).

To organize the results further we performed a two-dimensional hierarchical cluster analysis (Fig. 5a). One of the tightest clusters in the compound dimension includes BIRB-796, a p38 inhibitor, and BAY-43-9006, a RAF1 inhibitor (Table 1 and Fig. 5). The binding profile for BIRB-796 is largely a subset of that for BAY-43-9006, with 25 targets shared between them. Ten additional kinases bind BAY-43-9006, but not BIRB-796, and only three kinases bind BIRB-796 but not BAY-43-9006. The affinities of the two compounds for the shared targets, however, are very different (Supplementary Table 4 online). None of the four kinases with binding constants below 100 nM for BAY-43-9006 bind BIRB-796 with better than 1- μ M affinity. Conversely, only two of the eight kinases with binding constants below 100 nM for BIRB-796 bind BAY-43-9006 with better than 1- μ M affinity, and none with better than 100-nM affinity. Both molecules are substituted ureas with similarly spaced aromatic ring systems (Supplementary Table 1 online), showing that compounds based on the same structural scaffold can have closely related binding profiles even though they have been optimized for inhibition of different primary targets. Although the number of kinase inhibitors used here is not yet sufficient for general patterns to emerge, clustering of kinases based on small-molecule binding has the potential to reveal structural relationships between active sites that may not be obvious from an analysis of protein sequence²⁷.

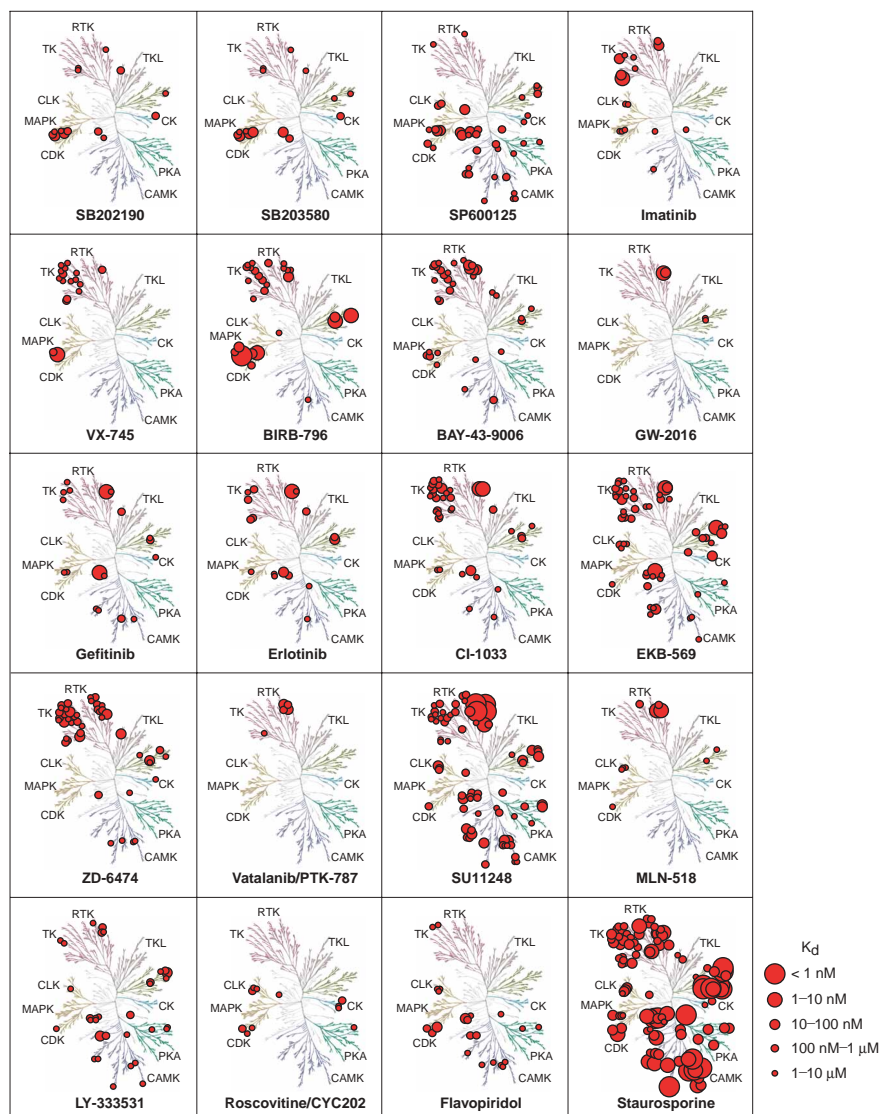


Figure 3 Specificity profiles of clinical kinase inhibitors. Kinase dendrograms were adapted³. TK, nonreceptor tyrosine kinases; RTK, receptor tyrosine kinases; TKL, tyrosine kinase-like kinases; CK, casein kinase family; PKA, protein kinase A family; CAMK, calcium/calmodulin dependent kinases; CDK, cyclin dependent kinases; MAPK, mitogen-activated protein kinases; CLK, CDK-like kinases. Circle size is proportional to binding affinity (on a \log_{10} scale). Binding constants were measured at least in duplicate for each interaction identified in the primary screen. Complete quantitative results are shown in Supplementary Table 4 online. The kinase dendrogram was adapted³ and is reproduced with permission from *Science* (<http://www.sciencemag.org>) and Cell Signaling Technology, Inc. (<http://www.cellsignal.com>).

Assays for imatinib-resistant mutated versions of the ABL kinase

Imatinib has been a very successful drug for the treatment of CML²⁸. Unfortunately, a considerable fraction of patients treated with the compound, including the majority of those with the advanced, blast-crisis form of the disease, eventually develop resistance^{29–31}. Resistance in most cases is due to either amplification of the *BCR-ABL* gene or to mutations in the ABL kinase that decrease sensitivity to imatinib³². There is thus a great need for second generation drugs that can inhibit the activity of imatinib-resistant mutant ABL kinases³³. To determine whether there are clinical kinase inhibitors capable of inhibiting these therapeutically relevant mutant kinases, we developed assays for six of the clinically observed mutant

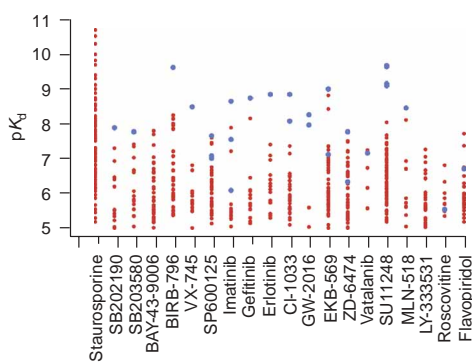


Figure 4 Distribution of binding constants. For each compound the pK_d ($-\log K_d$) was plotted for all targets identified. Primary targets, as shown in **Table 1**, are in blue, and off-targets in red. Staurosporine does not have a particular primary target or targets, and the primary targets for BAY-43-9006 (RAF1) and LY-333531 (PKC β) were not part of the assay panel.

ABL kinases^{29–31} and screened the set of 20 kinase inhibitors for binding to these variants (**Fig. 5b**).

One of the most commonly observed mutant forms in patients, T315I, is almost completely resistant to imatinib^{30,31,34,35}, consistent with the more than 1,000-fold difference in binding affinity between wild type and the T315I mutant observed here (**Fig. 5b**; **Supplementary Table 4** online). The E255K mutation confers greater than tenfold resistance in cell-based assays, whereas the Q252H, Y253F, M351T and H396P mutations have only moderate effects^{30,31,36}. Consistent with these observations, the E255K variant binds imatinib 50-fold more weakly than the wild-type kinase in our assays, whereas the remaining four mutations weaken binding only 6- to 30-fold. The relative susceptibility of these variant kinases to imatinib is therefore faithfully reflected in the binding constants measured here (**Fig. 5b**; **Supplementary Table 4** online), further illustrating that the ATP site-dependent binding assays reflect biologically relevant behavior of the kinases.

The 20 compounds tested fall into two classes based on their binding behavior against wild-type and mutated ABL. Ten of the compounds bound to all or most of the ABL variants, including wild type, whereas the other ten bound neither wild type nor any of the mutant forms (**Fig. 5b**; **Supplementary Table 4** online). The most striking finding is that the p38 inhibitor BIRB-796 binds ABL(T315I) with a ~ 40 nM binding constant (**Supplementary Table 4** online). Although several compounds have been described that can inhibit some of the imatinib-resistant ABL forms, none of these compounds effectively inhibit the important T315I mutant^{33,37–39}. These results highlight the fact that mutations present as polymorphisms or that emerge during tumor growth or in response to inhibitor treatment may result in a mutant protein that can be inhibited with compounds that do not bind well to the wild-type protein. This possibility can be exploited by assessing compound binding not only to a panel of wild-type kinases, but also to relevant variant forms.

A new target for imatinib

Although imatinib is not a promiscuous compound, our results reveal that in addition to the known targets ABL, platelet-derived growth factor receptor and KIT, it also binds tightly to the SRC-family tyrosine kinase LCK ($K_d = 62$ nM) (**Fig. 3**; **Supplementary Table 4** online). To further support this finding, we tested imatinib in a LCK enzyme activity assay, which showed the IC_{50} to be 160 nM at 10 μ M

ATP (Upstate Biotechnology; data not shown). Imatinib does not bind SRC itself, consistent with the lack of SRC inhibition reported previously⁴⁰, but does bind weakly to two additional SRC-family kinases, FRK and FYN (K_d of 3.5 and 5.5 μ M, respectively; **Supplementary Table 4** online). As an additional control, imatinib was tested in a FYN enzyme activity assay, which showed the IC_{50} to be 3.7 μ M at 10 μ M ATP (Invitrogen; data not shown), once again consistent with our binding measurements. SRC, FRK, FYN and LCK are closely related, and the fact that imatinib can discriminate between them presents an interesting subject for molecular recognition studies⁴¹.

LCK is a key regulator of T-cell maturation and activation and a potential target for immunosuppression⁴². It has been reported that treatment with imatinib suppresses T-cell proliferation^{43,44} and affects the LCK pathway⁴⁴, leading to the suggestion that imatinib may be clinically useful as an immunosuppressant⁴⁴. Our results may provide a molecular explanation for these observations.

Clinical EGFR mutations do not affect inhibitor binding

It was recently shown that the presence of specific somatic mutations in the EGFR tyrosine kinase in the vicinity of the ATP site correlates with sensitivity of NSCLC to the EGFR inhibitor gefitinib^{6,7}. This discovery at least partially explains the clinical observation that only a subset of patients respond to treatment with gefitinib and provides a means to identify those patients most likely to benefit from the drug. Two important questions are whether the mutations have a direct effect on the interaction between gefitinib and the EGFR, and whether the mutations are likely to sensitize tumors to treatment with other EGFR inhibitors currently in development.

To determine whether binding of gefitinib to the ATP site of EGFR is affected by the mutations, we developed assays for nine of the described NSCLC EGFR mutants and measured their binding affinities for gefitinib (**Supplementary Table 5** online). Gefitinib bound with similar affinity to wild type and mutant forms of EGFR, with the measured binding constants for all nine mutants within threefold of that for the wild type (**Fig. 6**; **Supplementary Table 5** online). To further determine whether other EGFR inhibitors, including several currently in clinical development, bind the EGFR mutant forms, we measured binding constants for seven additional compounds known to bind the ATP site of wild-type EGFR. We found very little difference between binding affinities for the wild type and any of the nine mutants for the inhibitors tested (**Fig. 6**; **Supplementary Table 5** online). For each compound, the affinities for all nine mutants were within approximately threefold of that for the wild type. The only exception was binding of SU-11464 to the G719C mutant, which was almost sevenfold weaker than binding to wild-type EGFR (**Fig. 6**; **Supplementary Table 5** online).

The mutations in the EGFR tyrosine kinase that confer sensitivity to gefitinib therefore do not fundamentally affect the intrinsic interaction between the ATP site of EGFR and small-molecule EGFR inhibitors. This contrasts with other activating catalytic domain mutations that have a profound effect on the interaction with imatinib and other inhibitors, such as mutations in KIT associated with mastocytosis⁴⁵. Compounds that discriminate between wild-type and mutant EGFRs may be able to achieve a therapeutic benefit while avoiding side effects such as the skin rash that has been observed with several EGFR inhibitors⁴⁶. That is to say, there is no privileged interaction between gefitinib and gefitinib-sensitizing EGFR mutants, and our results predict that tumors with gefitinib-sensitizing mutations should also respond to treatment with other small-molecule EGFR inhibitors. After our study was completed, it was reported that mutations similar to those found in gefitinib-sensitive patients are also

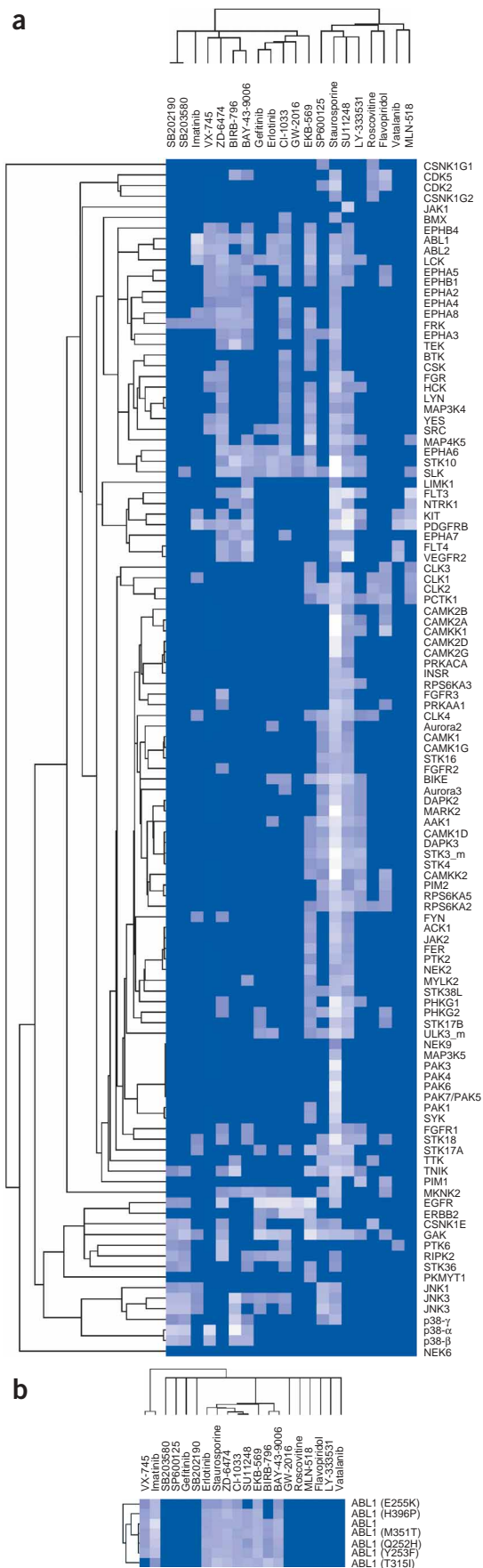


Figure 5 Hierarchical cluster analysis of specificity profiles. Lighter colors correspond to tighter interactions. **(a)** Twenty kinase inhibitors profiled against a panel of 113 different kinases. **(b)** The same compounds screened against a panel of six imatinib-resistant variants as well as the wild-type ABL kinase.

present in tumors from patients who have responded to treatment with erlotinib⁴⁷.

DISCUSSION

The binding assays described here have several significant advantages relative to traditional *in vitro* enzyme activity assays. First, the entire panel can be run in parallel in a single experiment. All of the assays are performed under the same conditions using similar reagents. Second, the entire set of kinases can be prepared in parallel in about 2 h immediately before use. Third, because of the low concentration of kinase used, the assays have a wide dynamic range and can measure binding affinities as low as 1–10 pM. Fourth, binding affinity provides a ‘common denominator’ that allows direct comparisons between all kinases in the panel. The assays are performed without added ATP or substrate and measure binding, rather than activity. The results, therefore, are not dependent on ATP concentration (or the K_m for ATP) or on the specific choice of substrate. Fifth, many protein kinases that do not fold efficiently when overexpressed in *E. coli* are amenable to our approach because of the extraordinary detection sensitivity of the assays; only a small fraction of the total expressed protein, less than 1%, needs to be properly folded to yield sufficient signal.

We have described a systematic small molecule–kinase interaction map for clinical kinase inhibitors. Integration of the information provided here with results from cell-based or animal studies, and ultimately with clinical observations, should enable a more complete understanding of the biological consequences of inhibiting particular combinations of kinases. Binding profiles for larger numbers of chemically diverse compounds, combined with the phenotypes elicited by these compounds in biological systems, will help identify kinases whose inhibition leads to adverse effects, kinases that are ‘safe’ to inhibit and combinations of kinases whose inhibition can have a synergistic beneficial effect in particular disease states. This knowledge should enable the development of inhibitors with ‘appropriate’ specificity that target multiple kinases involved in the disease process while avoiding kinases implicated in side effects. The ability to rapidly screen compounds against multiple kinases in parallel and the incorporation of specificity profiling during initial lead discovery and optimization should greatly facilitate and accelerate the drug development process.

The kinase binding profiles also provide valuable information to guide structural studies. In many cases kinases that tightly bind the same compound have no obvious sequence similarity (for example, p38 and ABL(T315I) binding to BIRB-796). In other cases, compounds can discriminate between kinases closely related by sequence, such as imatinib binding to LCK but not SRC. ABL and the imatinib-resistant ABL mutants are of particular structural interest because some compounds bind with good affinity to all forms (e.g., ZD-6474), whereas BIRB-796 has a strong preference for a particular mutant. Key insights should result from an analysis of selected co-crystal structures of kinase–compound combinations identified through profiling studies, and the large, uniform data set presented here should serve as a valuable training set for computation-based inhibitor design. Finally, the use of phage-tagged proteins in quantitative biochemical assays circumvents the need for conventional protein production and

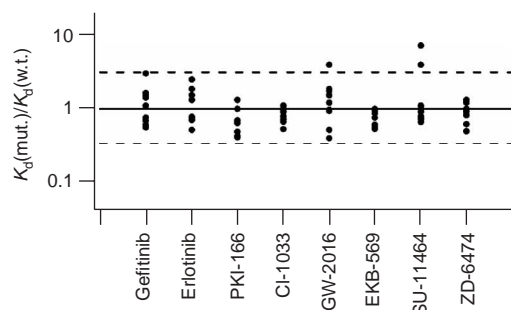


Figure 6 Relative binding affinities of EGFR inhibitors for wild type and mutant forms of EGFR. For each compound, the ratio of the K_d for each mutant relative to wild type was calculated. Dashed lines mark a threefold difference between binding constants for wild-type and mutant EGFRs ($K_d(\text{mut.})/K_d(\text{w.t.}) < 0.33$ or > 3).

purification, and should help reduce one of the major bottlenecks in modern proteomics and drug discovery research.

METHODS

Kinase cloning. Kinases were cloned in a modified version of the commercially available T7 Select 10–3 strain (Novagen). The head portion of each phage particle contains 415 copies of the major capsid protein, and in this system approximately one to ten of these are kinase fusion proteins. The fusion proteins are randomly distributed across the phage head surface. The N terminus of the kinase is fused to the C terminus of the capsid protein through a flexible peptide linker; the kinases are linked to the T7 phage particle but are not incorporated into the phage head. The fusion proteins are randomly incorporated, and therefore distributed across the phage head surface. In general, for single-domain kinases the entire coding region was cloned, whereas for large, multidomain proteins, such as receptor tyrosine kinases, the catalytic domain was cloned (Supplementary Table 6 online). Clones for each kinase were sequenced, compared to an appropriate reference sequence, changed by site-directed mutagenesis where necessary to exactly match the reference sequence throughout the kinase domain, and then transferred into the phage vector. Reference sequences for most of the kinases were obtained from the RefSeq database. Whenever available we chose a curated sequence as the reference ('NM' entries in RefSeq). For some of the kinases, there was evidence from genomic and/or EST sequences that RefSeq entries were not the most appropriate reference. In these cases alternative reference sequences consistent with genomic and EST sequences were obtained from GenBank or from Manning *et al.*³. Each kinase was fully resequenced after archiving to produce a clone collection that is highly curated and matched to human genome reference sequences.

Kinase assays. T7 kinase-tagged phage strains were grown in parallel in 24- or 96-well blocks in an *E. coli* host derived from the BL21 strain. *E. coli* were grown to log phase and infected with T7 phage from a frozen stock (multiplicity of infection ~ 0.1) and incubated with shaking at 32 °C until lysis (~ 90 min). The lysates were centrifuged (6,000g) and filtered (0.2 μm) to remove cell debris. Streptavidin-coated magnetic beads were treated with biotinylated small molecule ligands for 30 min at 25 °C to generate affinity resins for kinase assays. The liganded beads were blocked with excess biotin and washed with blocking buffer (SeaBlock (Pierce), 1% BSA, 0.05% Tween 20, 1 mM DTT) to remove unbound ligand and to reduce nonspecific phage binding. Binding reactions were assembled by combining phage lysates, liganded affinity beads and test compounds in 1 \times binding buffer (20% SeaBlock, 0.17 \times PBS, 0.05% Tween 20, 6 mM DTT). Test compounds were prepared as 1,000 \times stocks in DMSO and rapidly diluted into the aqueous environment (0.1% DMSO final). DMSO (0.1%) was added to control assays lacking a test compound. All reactions were carried out in polystyrene 96-well plates that had been pretreated with blocking buffer in a final volume of 0.1 ml. The assay plates were incubated at 25 °C with shaking for 1 h, long enough for

binding reactions to reach equilibrium (data not shown), and the affinity beads were washed four times with wash buffer (1 \times PBS, 0.05% Tween 20, 1 mM DTT) to remove unbound phage. After the final wash, the beads were resuspended in elution buffer (1 \times PBS, 0.05% Tween 20, 2 μM nonbiotinylated affinity ligand) and incubated at 25 °C with shaking for 30 min. The phage titer in the eluates was measured by standard plaque assays or by quantitative PCR.

Binding constant measurements. The equilibrium binding equations yield the following expression for the binding constant for the interaction between the free test compound and the kinase ($K_{d(\text{test})}$), assuming that the phage concentration is below $K_{d(\text{test})}$: $K_{d(\text{test})} = (K_{d(\text{probe})}/(K_{d(\text{probe})} + [\text{Probe}]]) \times [\text{test}]_{1/2}$. $K_{d(\text{probe})}$ is the binding constant for the interaction between the kinase and the immobilized ligand, [Probe] is the concentration of the immobilized ligand and $[\text{test}]_{1/2}$ is the concentration of the free test compound at the midpoint of the transition. If [Probe] is below $K_{d(\text{probe})}$ the expression simplifies to $K_{d(\text{test})} = [\text{test}]_{1/2}$. Under these conditions the binding constants measured for the interaction between kinases and test compounds ($K_{d(\text{test})}$) are therefore independent of the affinity of the immobilized ligand for the kinase ($K_{d(\text{probe})}$) (see Supplementary Notes online). T7 phage grow to a titer of 10^8 – 10^{10} plaque forming units (PFU)/ml, and the concentration of phage-tagged kinase in the binding reaction is therefore in the low picomolar range. The concentration of the immobilized ligand is kept in the low nanomolar range, below its binding constant for the kinase. Binding data were fit to the equation $\text{PFU} = L + ((H - L) \times (K_{d(\text{test})}/(K_{d(\text{test})} + [\text{test}])))$, where L is the lower baseline, H is the upper baseline, $K_{d(\text{test})}$ is the binding constant for the interaction between the test compound and the kinase, and [test] is the free test compound concentration. Binding constants measured in duplicate on the same day as part of the same experiment generally were within twofold. Duplicate measurements performed on separate days generally varied by no more than fourfold. Clustering and visualization was performed with Cluster 3.0 (M. Eisen, Stanford University) and Mapletree software (M. Eisen, Stanford University; L. Simirenko, Lawrence Berkeley National Lab). For kinase/compound combinations where no interaction was observed, the binding constant was arbitrarily set to 1 M. K_d values were converted to $\text{p}K_d$ ($-\log K_d$), and clustering was based on the Pearson correlation.

Note: Supplementary information is available on the Nature Biotechnology website.

ACKNOWLEDGMENTS

We thank Tony Hunter, Nicholas Lydon and Webster Cavenee for a critical reading of the manuscript and helpful discussions, Dan Lockhart for writing software tools to facilitate data analysis, David Austin for helpful suggestions regarding compound synthesis and Nicholas Olney and Victor Perez for expert technical assistance.

COMPETING INTERESTS STATEMENT

The authors declare competing financial interests (see the Nature Biotechnology website for details).

Received 16 September; accepted 20 December 2004

Published online at <http://www.nature.com/naturebiotechnology/>

- Dancey, J. & Sausville, E.A. Issues and progress with protein kinase inhibitors for cancer treatment. *Nat. Rev. Drug Discov.* **2**, 296–313 (2003).
- Cohen, P. Protein kinases—the major drug targets of the twenty-first century? *Nat. Rev. Drug Discov.* **1**, 309–315 (2002).
- Manning, G., Whyte, D.B., Martinez, R., Hunter, T. & Sudarsanam, S. The protein kinase complement of the human genome. *Science* **298**, 1912–1934 (2002).
- Davies, S.P., Reddy, H., Caivano, M. & Cohen, P. Specificity and mechanism of action of some commonly used protein kinase inhibitors. *Biochem. J.* **351**, 95–105 (2000).
- Bain, J., McLauchlan, H., Elliott, M. & Cohen, P. The specificities of protein kinase inhibitors: an update. *Biochem. J.* **371**, 199–204 (2003).
- Lynch, T.J. *et al.* Activating mutations in the epidermal growth factor receptor underlying responsiveness of non-small-cell lung cancer to gefitinib. *N. Engl. J. Med.* **350**, 2129–2139 (2004).
- Paez, J.G. *et al.* EGFR mutations in lung cancer: correlation with clinical response to gefitinib therapy. *Science* **304**, 1497–1500 (2004).
- Sche, P.P., McKenzie, K.M., White, J.D. & Austin, D.J. Display cloning: functional identification of natural product receptors using cDNA-phage display. *Chem. Biol.* **6**, 707–716 (1999).

9. Kumar, S., Boehm, J. & Lee, J.C. p38 MAP kinases: key signalling molecules as therapeutic targets for inflammatory diseases. *Nat. Rev. Drug Discov.* **2**, 717–726 (2003).
10. Lee, J.C. *et al.* A protein kinase involved in the regulation of inflammatory cytokine biosynthesis. *Nature* **372**, 739–746 (1994).
11. Godi, K. *et al.* An efficient proteomics method to identify the cellular targets of protein kinase inhibitors. *Proc. Natl. Acad. Sci. USA* **100**, 15434–15439 (2003).
12. Tong, L. *et al.* A highly specific inhibitor of human p38 MAP kinase binds in the ATP pocket. *Nat. Struct. Biol.* **4**, 311–316 (1997).
13. Pargellis, C. *et al.* Inhibition of p38 MAP kinase by utilizing a novel allosteric binding site. *Nat. Struct. Biol.* **9**, 268–272 (2002).
14. Fitzgerald, C.E. *et al.* Structural basis for p38alpha MAP kinase quinazolinone and pyridol-pyrimidine inhibitor specificity. *Nat. Struct. Biol.* **10**, 764–769 (2003).
15. Gray, N.S. *et al.* Exploiting chemical libraries, structure, and genomics in the search for kinase inhibitors. *Science* **281**, 533–538 (1998).
16. Meggio, F. *et al.* Different susceptibility of protein kinases to staurosporine inhibition. Kinetic studies and molecular bases for the resistance of protein kinase CK2. *Eur. J. Biochem.* **234**, 317–322 (1995).
17. Bennett, B.L. *et al.* SP600125, an anthranyprazolone inhibitor of Jun N-terminal kinase. *Proc. Natl. Acad. Sci. USA* **98**, 13681–13686 (2001).
18. Buchdunger, E., Matter, A. & Druker, B.J. Bcr-Abl inhibition as a modality of CML therapeutics. *Biochim. Biophys. Acta* **1551**, M11–M18 (2001).
19. Wakeling, A.E. *et al.* ZD1839 (gefitinib): an orally active inhibitor of epidermal growth factor signaling with potential for cancer therapy. *Cancer Res.* **62**, 5749–5754 (2002).
20. Moyer, J.D. *et al.* Induction of apoptosis and cell cycle arrest by CP-358,774, an inhibitor of epidermal growth factor receptor tyrosine kinase. *Cancer Res.* **57**, 4838–4848 (1997).
21. Allen, L.F., Lenehan, P.F., Eiseman, I.A., Elliott, W.L. & Fry, D.W. Potential benefits of the irreversible pan-erbB inhibitor, CI-1033, in the treatment of breast cancer. *Semin. Oncol.* **29**, 11–21 (2002).
22. Rusnak, D.W. *et al.* The effects of the novel, reversible epidermal growth factor receptor/ErbB-2 tyrosine kinase inhibitor, GW2016, on the growth of human normal and tumor-derived cell lines *in vitro* and *in vivo*. *Mol. Cancer Ther.* **1**, 85–94 (2001).
23. Torrance, C.J. *et al.* Combinatorial chemoprevention of intestinal neoplasia. *Nat. Med.* **6**, 1024–1028 (2000).
24. Wedge, S.R. *et al.* ZD6474 inhibits vascular endothelial growth factor signaling, angiogenesis, and tumor growth following oral administration. *Cancer Res.* **62**, 4645–4655 (2002).
25. Wood, J.M. *et al.* PTK787/ZK 222584, a novel and potent inhibitor of vascular endothelial growth factor receptor tyrosine kinases, impairs vascular endothelial growth factor-induced responses and tumor growth after oral administration. *Cancer Res.* **60**, 2178–2189 (2000).
26. Kelly, L.M. *et al.* CT53518, a novel selective FLT3 antagonist for the treatment of acute myelogenous leukemia (AML). *Cancer Cell* **1**, 421–432 (2002).
27. Vieth, M. *et al.* Kinomics-structural biology and chemogenomics of kinase inhibitors and targets. *Biochim. Biophys. Acta* **1697**, 243–257 (2004).
28. Druker, B.J. Perspectives on the development of a molecularly targeted agent. *Cancer Cell* **1**, 31–36 (2002).
29. Gorre, M.E. *et al.* Clinical resistance to STI-571 cancer therapy caused by BCR-ABL gene mutation or amplification. *Science* **293**, 876–880 (2001).
30. von Bubnoff, N., Schneller, F., Peschel, C. & Duyster, J. *BCR-ABL* gene mutations in relation to clinical resistance of Philadelphia-chromosome-positive leukaemia to STI571: a prospective study. *Lancet* **359**, 487–491 (2002).
31. Shah, N.P. *et al.* Multiple BCR-ABL kinase domain mutations confer polyclonal resistance to the tyrosine kinase inhibitor imatinib (STI571) in chronic phase and blast crisis chronic myeloid leukemia. *Cancer Cell* **2**, 117–125 (2002).
32. Gambacorti-Passerini, C.B. *et al.* Molecular mechanisms of resistance to imatinib in Philadelphia-chromosome-positive leukaemias. *Lancet Oncol.* **4**, 75–85 (2003).
33. Shah, N.P. *et al.* Overriding imatinib resistance with a novel ABL kinase inhibitor. *Science* **305**, 399–401 (2004).
34. Branford, S. *et al.* High frequency of point mutations clustered within the adenosine triphosphate-binding region of BCR/ABL in patients with chronic myeloid leukemia or Ph-positive acute lymphoblastic leukemia who develop imatinib (STI571) resistance. *Blood* **99**, 3472–3475 (2002).
35. Azam, M., Latek, R.R. & Daley, G.Q. Mechanisms of autoinhibition and STI-571/imatinib resistance revealed by mutagenesis of BCR-ABL. *Cell* **112**, 831–843 (2003).
36. Roumiantsev, S. *et al.* Clinical resistance to the kinase inhibitor STI-571 in chronic myeloid leukemia by mutation of Tyr-253 in the Abl kinase domain P-loop. *Proc. Natl. Acad. Sci. USA* **99**, 10700–10705 (2002).
37. Warmuth, M. *et al.* Dual-specific Src and Abl kinase inhibitors, PP1 and CGP76030, inhibit growth and survival of cells expressing imatinib mesylate-resistant Bcr-Abl kinases. *Blood* **101**, 664–672 (2003).
38. La Rosee, P., Corbin, A.S., Stoffregen, E.P., Deininger, M.W. & Druker, B.J. Activity of the Bcr-Abl kinase inhibitor PD180970 against clinically relevant Bcr-Abl isoforms that cause resistance to imatinib mesylate (imatinib, STI571). *Cancer Res.* **62**, 7149–7153 (2002).
39. Huron, D.R. *et al.* A novel pyridopyrimidine inhibitor of abl kinase is a picomolar inhibitor of Bcr-abl-driven K562 cells and is effective against STI571-resistant Bcr-abl mutants. *Clin. Cancer Res.* **9**, 1267–1273 (2003).
40. Druker, B.J. *et al.* Effects of a selective inhibitor of the Abl tyrosine kinase on the growth of Bcr-Abl positive cells. *Nat. Med.* **2**, 561–566 (1996).
41. Nagar, B. *et al.* Crystal structures of the kinase domain of c-Abl in complex with the small molecule inhibitors PD173955 and imatinib (STI-571). *Cancer Res.* **62**, 4236–4243 (2002).
42. Goldberg, D.R. *et al.* Optimization of 2-phenylaminoimidazo[4,5-h]isoquinolin-9-ones: orally active inhibitors of Ick kinase. *J. Med. Chem.* **46**, 1337–1349 (2003).
43. Mattiuzzi, G.N. *et al.* Development of Varicella-Zoster virus infection in patients with chronic myelogenous leukemia treated with imatinib mesylate. *Clin. Cancer Res.* **9**, 976–980 (2003).
44. Dietz, A.B. *et al.* imatinib mesylate inhibits T-cell proliferation *in vitro* and delayed-type hypersensitivity *in vivo*. *Blood* **104**, 1094–1099 (2004).
45. Ma, Y. *et al.* The c-KIT mutation causing human mastocytosis is resistant to STI571 and other KIT kinase inhibitors; kinases with enzymatic site mutations show different inhibitor sensitivity profiles than wild-type kinases and those with regulatory-type mutations. *Blood* **99**, 1741–1744 (2002).
46. Lynch, T.J. *et al.* Novel agents in the treatment of lung cancer: conference summary statement. *Clin. Cancer Res.* **10**, 4199s–4204s (2004).
47. Pao, W. *et al.* EGF receptor gene mutations are common in lung cancers from “never smokers” and are associated with sensitivity of tumors to gefitinib and erlotinib. *Proc. Natl. Acad. Sci. USA* **101**, 13306–13311 (2004).